Biochemistry

 Volume 41, Number 42 October 22, 2002

Accelerated Publications

Three-Dimensional Structure of Human Tryptophan Hydroxylase and Its Implications for the Biosynthesis of the Neurotransmitters Serotonin and Melatonin[†,‡]

Lin Wang,[§] Heidi Erlandsen,[§] Jan Haavik,[||] Per M. Knappskog,[⊥] and Raymond C. Stevens*[,§]

Department of Molecular Biology, The Scripps Research Institute, 10550 North Torrey Pines Road, La Jolla, California 92037, Department of Biochemistry and Molecular Biology, University of Bergen, Årstadveien 19, N-5009 Bergen, Norway, and Center of Medical Genetics and Molecular Medicine, University of Bergen, Haukeland Hospital, N-5021 Bergen, Norway

Received August 2, 2002; Revised Manuscript Received September 4, 2002

ABSTRACT: Tryptophan hydroxylase oxidizes L-tryptophan to 5-hydroxy-L-tryptophan in the rate-determining step of serotonin biosynthesis. We have determined the X-ray crystal structure (1.7 Å) of a truncated functional form of human tryptophan hydroxylase with the bound cofactor analogue 7,8-dihydro-L-biopterin, providing the first atomic-resolution information for the catalytic domain of this important enzyme. Comparison of the three-dimensional structures of all three members of the aromatic amino acid hydroxylase family—tyrosine hydroxylase, phenylalanine hydroxylase, and tryptophan hydroxylase—reveals important differences at the active sites.

Serotonin (5-hydroxytryptamine) is a hormone and neurotransmitter that is widely distributed in nature. In animals, it serves regulatory purposes in the central nervous system (CNS)[1] and in several peripheral organs. In the human brain, serotonin is involved in numerous physiological functions, including sleep, pain, appetite, sexual behavior, and mood, and is the precursor of the pineal hormone melatonin. The first and rate-limiting step in serotonin biosynthesis is catalyzed by tryptophan hydroxylase (TrpOH) (Scheme 1), which uses (6*R*)-L-*erythro*-5,6,7,8-tetrahydrobiopterin (BH_4) and dioxygen cofactors along with the dietary essential amino acid substrate L-tryptophan (L-Trp) (*1*), in generating 5-hydroxy-L-tryptophan that is converted to 5-hydroxytryptamine (5-HT or serotonin) by aromatic amino acid decarboxylase.

Multiple lines of evidence suggest that serotonergic neurotransmission is changed in psychiatric conditions such as depression, schizophrenia, obsessive-compulsive disorders, aggression, and suicide. Many studies have revealed associations between TrpOH gene sequence variants and various

[†] This work was supported in part by the National Institutes of Health (Grant HD38718), the Locus on Neuroscience, and The Research Council of Norway.

[‡] The coordinates have been deposited with the Protein Data Bank as entry 1MLW.

* To whom correspondence should be addressed. E-mail: stevens@scripps.edu. Fax: (858) 784-9483.

[§] The Scripps Research Institute.

[||] University of Bergen.

[⊥] Haukeland Hospital.

[1] Abbreviations: CNS, central nervous system; TrpOH, tryptophan hydroxylase; BH_4, (6*R*)-L-*erythro*-5,6,7,8-tetrahydrobiopterin; L-Trp, L-tryptophan; 5-HT, 5-hydroxytryptamine (serotonin); SSRIs, selective serotonin reuptake inhibitors; AAOHs, aromatic amino acid hydroxylases; BBB, blood−brain barrier; TyrOH, tyrosine hydroxylase; PheOH, phenylalanine hydroxylase; hTrpOH, human tryptophan hydroxylase; BH_2, 7,8-dihydro-L-biopterin; hPheOH, human phenylalanine hydroxylase; rTyrOH, rat tyrosine hydroxylase; NMR, nuclear magnetic resonance.

10.1021/bi026561f CCC: $22.00
Published on Web 09/26/2002

Scheme 1: Serotonin and Melatonin Biosynthesis Pathway[a]

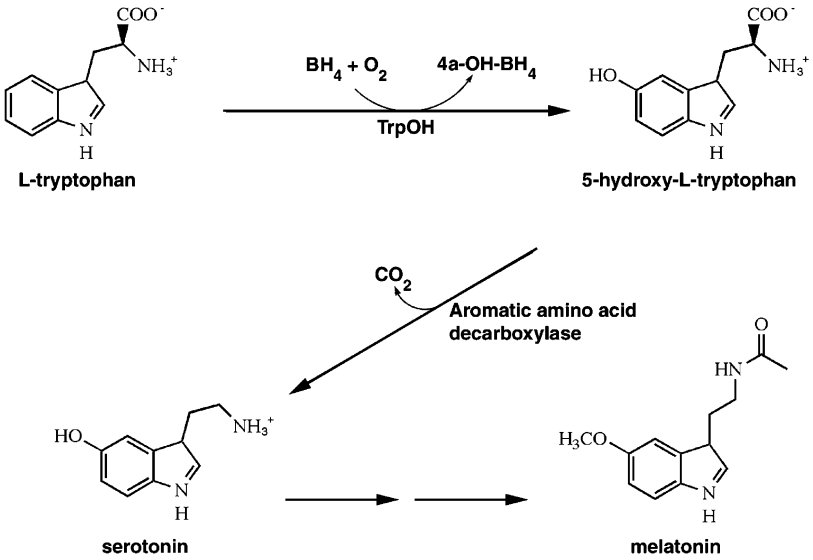

[a] The rate-limiting step of serotonin biosynthesis is catalyzed by tryptophan hydroxylase (TrpOH).

psychiatric conditions; however, most mutations are found in noncoding regions of the TrpOH sequence, and limited information about their functional consequences is available (*1*, *2*). In humans, the stimulation of serotonin production by administration of tryptophan has an antidepressant effect and inhibition of TrpOH may precipitate depression (*1*, *3*). Recently, TrpOH expression was found to be upregulated by chronic treatment with selective serotonin reuptake inhibitors (SSRIs), providing a further link between the antidepressant effect and TrpOH activity (*4*). Tryptophan analogues such as *p*-chlorophenylalanine and *p*-ethynylphenylalanine are competitive inhibitors of TrpOH, and are used to study the *in vivo* effect of serotonin on brain functions (*5*, *6*). Attempts to design more potent TrpOH inhibitors have so far been largely unsuccessful, partly due to an incomplete understanding of the enzyme binding site. In addition, tetrahydrobiopterin (BH_4) is an obligatory cofactor for the aromatic amino acid hydroxylases (AAOHs), and has previously been tested as an antidepressant with inconsistent results, possibly due to its poor blood−brain barrier (BBB) permeability and lack of stability (*7*). Therefore, synthetic derivatives of BH_4 with increased stability, BBB permeability, and cofactor efficiency could be potential antidepressants. Hence, new and more selective TrpOH inhibitors and BH_4 cofactor analogues can be devised on the basis of the three-dimensional structure of the catalytic domain of TrpOH presented here.

In addition to its role in the nervous system, serotonin is important for smooth muscle contraction, hemostasis, and intestinal function (*8*). Interestingly, intestinal dysfunction is the most consistent clinical finding in patients with high-titer inhibitory autoantibodies against (peripheral) TrpOH (*9*). Such patients could possibly benefit from treatments that improve serotonin production, such as the administration of the aforementioned BH_4 cofactor analogues. Conversely, selective serotonin antagonists are used in the treatment of irritable bowel syndrome and drug-induced nausea/emesis, but many of these drugs have toxic side effects (*10*). Therefore, an additional therapeutic approach would be to reduce the intestinal level of serotonin with the design of TrpOH specific inhibitors that act locally.

Crystallization and structural analyses have previously been reported for the other AAOHs tyrosine hydroxylase (TyrOH) and phenylalanine hydroxylase (PheOH) (*11*−*18*). However, TrpOH has hitherto resisted crystallization. This is partly due to the low abundance of TrpOH in mammalian tissues and the tendency of the full-length enzyme to aggregate when expressed either eukaryotically or prokaryotically. The human TrpOH (hTrpOH) structure presented here represents a framework for understanding the role of and enabling the modulation of the function of hTrpOH in normalcy and disease.

EXPERIMENTAL PROCEDURES

Protein Expression, Purification, and Crystallization. The ΔNH102-ΔCOOH402 human TrpOH gene was cloned into the pET23a vector (six-His C-terminal fusion) (Novagen) between restriction sites *Nde*I and *Xho*I, and overexpressed using BL21(DE3) cells in LB medium with 100 μg/mL ampicillin and 0.2 mM $Fe(NH_4)_2(SO_4)_2$ at 37 °C to an OD_{600} of ∼0.8, with 1 mM IPTG induction at 25 °C for 15 h. The cell pellet was lysed in buffer [50 mM Tris (pH 8.0), 400 mM NaCl, 3 mM methionine (to prevent oxidative degradation of proteins), 1 mM $MgCl_2$, 5% glycerol, DNase, EDTA-free protease inhibitor cocktail (Complete EDTA-free; Roche Diagnostics GmbH), and 1 mM PMSF]. Soluble TrpOH was purified by FPLC with an Applied Biosystems Poros MC column (running buffer consisting of 50 mM Tris, 400 mM NaCl, 3 mM methionine, 5% glycerol, 1 mM PMSF, and 20 mM imidazole; elution buffer was the same as running buffer but with 500 mM imidazole) and a Poros HQ column, with TrpOH collected in the HQ column flow-through (running buffer consisting of 50 mM Tris, 3 mM methionine, and 5% glycerol (pH 8.0); the TrpOH fraction from the MC column was diluted with HQ running buffer to bring the NaCl concentration to 50 mM; column regeneration buffer was the same as running buffer but with 1 M NaCl). For crystallization-quality TrpOH, a second MC column was used (same conditions as first purification step). Before the crystallization trays were set up, the TrpOH solution was dialyzed into 25 mM MES buffer (pH 6) containing 100 mM

Table 1: Data Collection and Refinement Statistics

data collection	
resolution (Å)	50.0−1.71 (1.77−1.71)
space group	$P2_12_12_1$
cell constants (Å)	$a = 47.78$, $b = 57.33$, $c = 109.41$
cell angles (deg)	$\alpha = \beta = \gamma = 90$
completeness (%)	99.2 (98.4)
no. of total observations	320396
no. of unique observations	32923 (3215)
redundancy	9 (9)
R_{sym} (%)[a,b]	9.9 (99.1)
molecular replacement	
resolution range (Å)	12−4
R-factor	51.7
correlation coefficient	0.344
refinement	
resolution range (Å)	20.0−1.71
no. of reflections (working set/test set)	30181/1347
R_{cryst} (%)[c]	20.7
R_{free} (%)[c]	23.1
rms deviation from ideal geometry	
bond lengths (Å)	0.005
bond angles (deg)	1.2
dihedral angles (deg)	20.9
improper angles (deg)	0.79
estimated coordinate error (from Luzzati plot) (Å)	0.20
estimated coordinate error (from SIGMAA) (Å)	0.18
no. of atoms in model	
protein	2605
ligands and ions	18
waters	242

[a] Numbers in parentheses are for the highest-resolution shell. [b] $R_{sym} = \sum|I - \langle I\rangle|/\sum I$. [c] $R_{cryst} = \sum||F_{obs}| - |F_{calc}||/\sum|F_{obs}|$, where F_{obs} and F_{calc} are the observed and calculated structure factors, respectively. $R_{free} = \sum||F_{obs}| - |F_{calc}||/\sum|F_{obs}|$ for 10% of the data not used at any stage of structural refinement.

NaCl, 3 mM methionine, and 5% glycerol, with any precipitate that formed being removed by centrifugation. The purity of the protein was >99% as determined by sodium dodecyl sulfate−polyacrylamide gel electrophoresis (SDS−PAGE) with Coomassie Brilliant Blue staining. Purified doubly truncated (ΔNH102-ΔCOOH402) human TrpOH displays activity comparable to that of a singly truncated form (ΔNH 90) of TrpOH (*19*) and has activity similar to that of a different doubly truncated form which has been characterized previously (ΔNH102-ΔCOOH416) (*20*).

A crystallization screening robot (Syrrx Inc., San Diego, CA) was used for the initial screening against 1152 different crystallization conditions (at 4 and 25 °C) using 50 nL protein droplets. After optimization of the initial crystallization conditions found with the robot, cocrystals of native TrpOH in complex with the cofactor analogue BH_2 were grown at 4 °C by sitting drop vapor diffusion using 16−18% MPEG5K and 25−40 mM MES (pH 6.0); native TrpOH was incubated with 6 mM BH_2 for 30 min on ice before crystallization experiments were set up. The crystals were cryoprotected in 25% (v/v) ethylene glycol and mother liquor before being flash-cooled in liquid nitrogen.

Structure Solution and Refinement. Diffraction data were collected at Stanford Synchrotron Radiation Laboratory (SSRL) beamline 9-1 and processed and reduced using HKL2000 and SCALEPACK (*21*). The TrpOH−Fe−BH_2 complex crystallized in space group $P2_12_12_1$. Data collection and processing statistics are given in Table 1.

Molecular replacement was carried out with the program EPMR (*22*). Initial phases for the TrpOH−Fe−BH_2 complex were obtained using human doubly truncated PheOH (PheOH residues 117−424; PDB entry 1PAH) as a search model. The structure was refined using CNS (*23*), with cycles of rigid-body, simulated annealing, *B*-grouped factor refinement, and energy minimization. Manual adjustment and rebuilding were performed using the program O (*24*). At the last stages of refinement, iron, BH_2, and waters were added to the structure and refined along with the protein. The quality of the refined model is shown in Table 1 as well as in the Supporting Information; 94.1% of the TrpOH residues are in the most favored regions of the Ramachandran plot, with 5.1% in the additionally allowed regions and 0.8% [two residues (Tyr125 and Thr367)] in the generously allowed regions.

RESULTS AND DISCUSSION

Kinetic Analysis of Doubly Truncated TrpOH (ΔNH102-ΔCOOH402). The doubly truncated TrpOH (ΔNH102-ΔCOOH402) used in this study is catalytically active, with a V_{max} value of 34.6 ± 0.7 nmol min^{-1} (mg of protein)$^{-1}$ and K_m values of 26.5 ± 2.0 μM for BH_4 and 7.8 ± 2.2 μM for L-tryptophan. Substrate inhibition by tryptophan was observed above 70 μM.

Overall Structure of Human TrpOH. The structure of doubly truncated human TrpOH (ΔNH102-ΔCOOH402) containing a 7,8-dihydro-L-biopterin (BH_2) oxidized cofactor analogue at the active site in addition to ferric iron was determined to 1.7 Å resolution using molecular replacement, with human PheOH as a search model (PDB entry 1PAH). TrpOH has a catalytic core of mixed α and β structure, similar to that of hPheOH and rTyrOH (Figure 1), as well as *Chromobacterium violaceum* PheOH (*11*, *14*, *17*, *18*). The root-mean-square (rms) structural deviations of doubly truncated hTrpOH to the corresponding regions of PheOH (PDB entry 1PAH; level of sequence identity of 65%) and TyrOH (PDB entry 1TOH; level of sequence identity of 62%) are 1.0 and 0.9 Å, respectively [calculated with the program TOP (*25*)]. Doubly truncated hTrpOH crystallizes as a monomer (M_w = 35 600 Da), as would be expected due to truncation of the region responsible for dimer and tetramer formation in the homologous enzymes TyrOH and PheOH (see the alignments in Figure 1b) (*13*). The monomeric state of doubly truncated hTrpOH was confirmed by light-scattering analysis. The approximate dimensions of the hTrpOH monomer are 48 Å × 48 Å × 35 Å.

hTrpOH Active Site. Although most of the residues that directly bind the iron and cofactor are conserved among the aromatic amino acid hydroxylases (Figure 1b), a few notable exceptions are present in hTrpOH. The lining of the hTrpOH active site crevice has a number of different amino acids compared to PheOH and TyrOH.

The hTrpOH active site consists of an approximately 9 Å deep and 10 Å wide cavity. Connected to the active site opening is an ~12 Å long and ~7 Å wide channel. Molecular docking studies on a modeled TrpOH structure have determined that this channel is where tryptophan most likely binds (*19*). Lining the active site channel are two loops (residues 263−269 and residues 363−372), with the latter loop having poor electron density and high *B*-factors. Interestingly, the

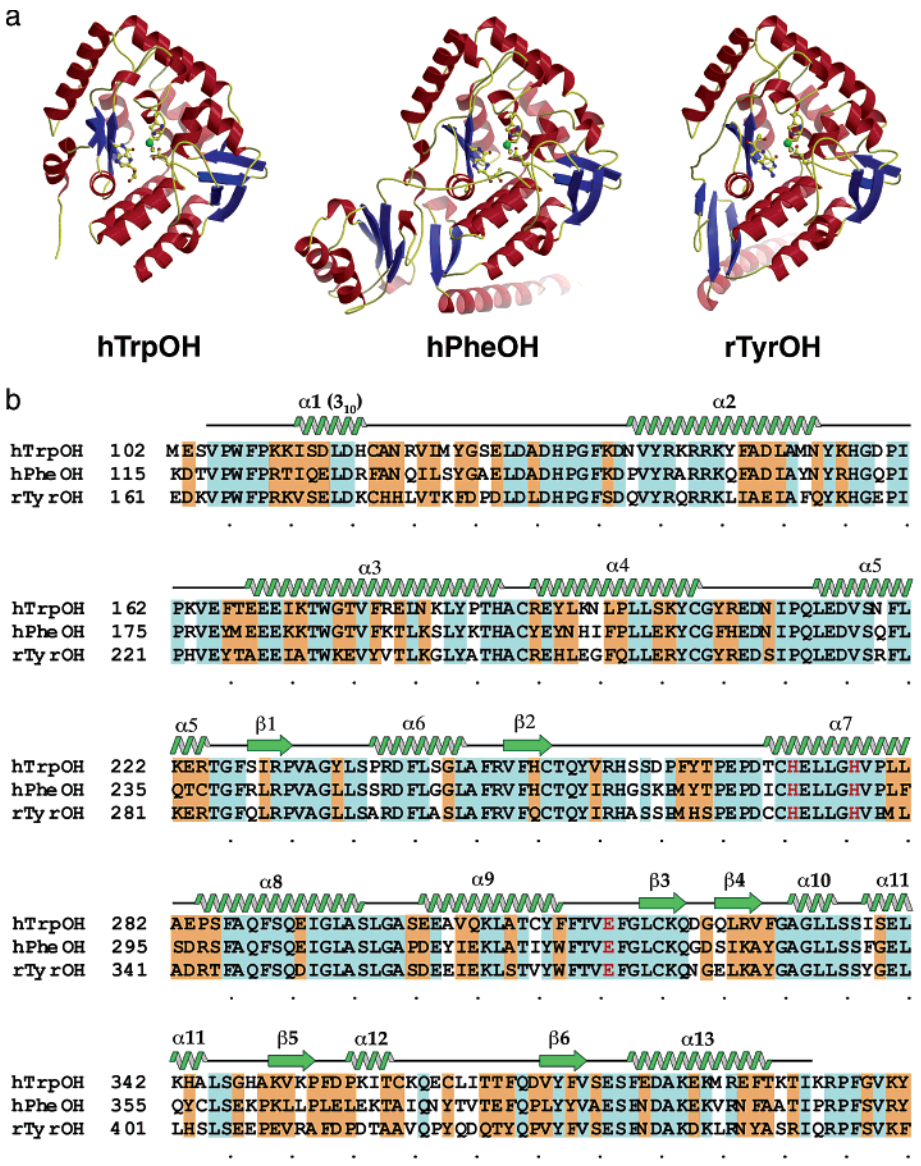

FIGURE 1: (a) Ribbon diagrams of hTrpOH (left), human PheOH (center) (composite model based on PDB entries 2PAH and 2PHM), and rTyrOH (right) (PDB entry 2TOH). The α-helices of the respective catalytic domains are colored red, the *β*-strands blue, and the coiled regions yellow. The active site iron is shown as a green sphere, and the bound 7,8-BH_2 cofactor is shown as a ball-and-stick model with carbon atoms in yellow, oxygen atoms in red, and nitrogen atoms in blue. (b) Sequence alignment of the three aromatic amino acid hydroxylases that have been structurally characterized by X-ray crystallography to date (rat PheOH sequence not shown): human tryptophan hydroxylase (hTrpOH), human phenylalanine hydroxylase (hPheOH), and rat tyrosine hydroxylase (rTyrOH). The secondary structure assignment that is shown is for hTrpOH, and was generated using the program DSSP (*33*). Secondary structural elements are indicated and numbered sequentially starting from the N-terminus. Blue-colored boxes surround the identical residues in all three hydroxylases, whereas residues identical in two of the three hydroxylases are surrounded by orange boxes. The three residues involved in iron binding at the active site are colored red.

largest positional differences observed in the TrpOH structure, as compared to the rTyrOH and hPheOH structures, are found in these two loops close to the substrate binding region. In addition, as discussed in the following section, the respective cofactor binding regions, located between residues 123 and 129 in TrpOH, are different for the three AAOH structures. Although the conformations of these loop regions are varied in the three different AAOHs, the positions of the two TrpOH side chains believed to be involved in determining substrate specificity, Phe313 (*19*, *26*) and Ile366 (*27*), can be superimposed with the positions of the corresponding residues in hPheOH (Trp326 and Val379, respectively) and rTyrOH (Trp372 and Asp425, respectively).

As predicted in previous studies (*1*, *28*, *29*), hTrpOH contains a catalytic Fe(III) atom ~13 Å below the surface, on the floor of the active site, at the intersection of the channel and the opening to the active site, and coordinated to His272 (N−Fe distance of 2.1 Å), His277 (N−Fe distance of 2.0 Å), and one carboxyl oxygen atom of Glu317 (O−Fe distance of 2.4 Å). Well-defined electron density is also observed for three water molecules coordinated to the iron: Wat1 (axial to His272)−Fe distance of 2.2 Å, Wat2 (axial to His277)−Fe distance of 2.3 Å, and Wat3 (axial to Glu317)−Fe distance of 2.2 Å. The iron is approximately octahedrally coordinated, similar to what was seen in the ferric doubly truncated hPheOH structure (*14*, *16*) (Figure 2). In contrast, only five iron ligands were observed in ferric rTyrOH (*11*).

hTrpOH Cofactor Binding Site. Due to the key roles of the aromatic amino acid hydroxylases (AAOHs) in catalyzing

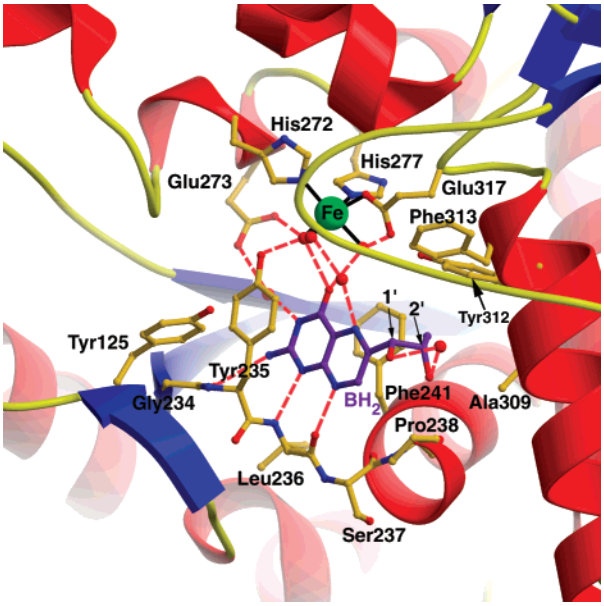

FIGURE 2: Active site of the iron- and cofactor (7,8-dihydro-L-biopterin)-bound form of hTrpOH. The residues involved in iron binding are shown for active site identification. The region mainly responsible for cofactor binding (Gly234−Pro238) is shown in ball-and-stick mode for clarification of hydrogen bonding interactions with the pterin. The α-helices of the catalytic domain are colored red, the β-strands blue, and the coiled regions yellow. The active site iron is shown as a green sphere, and the bound 7,8-BH_2 cofactor is shown as a ball-and-stick model with carbon atoms in purple, oxygen atoms in red, and nitrogen atoms in blue; the dihydroxypropyl atom numbering is indicated. Hydrogen bonds are represented by dashed red lines between atoms, and iron coordination is represented by black solid lines.

neurotransmitter biosyntheses, numerous studies have designed small molecules that selectively enhance or inhibit the function of the AAOHs. For example, many synthetic tetrahydropteridines have displayed catalytic efficiencies higher than that of the natural BH_4 cofactor (*30*). Crystal structures of hPheOH and rTyrOH with either BH_2 or BH_4 bound have revealed cofactor binding determinants, and recent NMR studies have indicated that the conformation of BH_2 is different when bound to TrpOH versus the other AAOHs (*19*). Thus, structural analysis of the hTrpOH cofactor binding site provides differences in cofactor binding that can be utilized in structure-based design of improved cofactor analogues.

In the oxidized cofactor 7,8-dihydro-L-biopterin (BH_2) form of ferric hTrpOH, the cofactor binds in the same orientation and position as in hPheOH (*16*, *31*). However, important differences are found in hTrpOH; first, Tyr235 forms a second π-stacking interaction on the opposite face of the pterin ring as compared to Phe241 (see the next paragraph), sandwiching the pterin ring close to the iron (Figure 2). Tyr235 is conserved in all known TrpOHs, whereas in both PheOH and TyrOH, it is a smaller hydrophobic leucine; the leucine side chains in hPheOH and rTyrOH are located on the opposite side of the pterin as compared to those of Phe241. When the residue is mutated into an alanine (Y235A) or a leucine (Y235L), the mutant TrpOH protein exhibited reduced specific activity (~5%) compared to that of the wild type (*32*) and an increased K_m for the L-Trp substrate (13- and 2-fold, respectively, for the Y235A and Y235L mutants) but a somewhat lowered K_m for BH_4 (2-fold lower K_m in the case of the Y235A mutant). Thus, it appears as if Tyr235 may be involved in both substrate binding and cofactor binding. A crystal structure of a ternary complex between TrpOH, a substrate analogue, and BH_4 under reducing and anaerobic conditions may confirm this hypothesis.

Second, in the region of residues 123−129 of hTrpOH, Tyr125 π-stacks onto Tyr235, forming an angle of 90° with respect to the aromatic rings (3.8 Å). The corresponding residue is a tyrosine in most TrpOHs and PheOHs (and is a phenylalanine in most TyrOHs), but in the hPheOH structure, this tyrosine is positioned toward the surface, instead of into the active site. These differences in the AAOH cofactor binding sites are consistent with the distinct cofactor structural preferences displayed by the three enzymes, even though they share a common reaction mechanism (*29*).

As previously mentioned, the pterin π-stacks on Phe241 (at an approximate distance of 3.8 Å) and Tyr235 (at an approximate distance of 3.6 Å), forming hydrogen bonds to Gly234 [BH_2(NH_2)−Gly234(C═O) distance of 3.1 Å] and Leu236 [BH_2(N1)−Leu236(N) distance of 3.0 Å, BH_2(N8)−Leu236(C═O) distance of 2.7 Å]. The pterin O4 atom is also hydrogen bonded to two of the three water molecules coordinated to the iron, with distances of 2.4 and 2.8 Å. The O4 atom of the pterin ring is 3.3 Å away from the third water molecule coordinated to the iron. Glu273 also forms two water-mediated hydrogen bonds to the pterin (one of which is the iron ligand Wat3) at the following distances: BH_2(NH_2)−Wat4−Glu273(Oϵ2) distances of 2.9 and 2.7 Å and BH_2(O4)−Wat3−Glu273(Oϵ1) distance of 2.8 and 2.7 Å, respectively. The pterin N3 atom also forms a hydrogen bond to Wat4 (2.8 Å).

Pro238 is an important sequence difference in hTrpOH. The analogous position in hPheOH, Ser251, forms hydrogen bonds to the dihydroxypropyl side chain in the ferrous BH_4-bound hPheOH structure (*31*). In hTrpOH, Pro238 is 3.6 Å away from the BH_2 dihydroxypropyl side chain 1′-OH atom, which leads to a change in the conformation of the dihydroxypropyl side chain in hTrpOH as compared to hPheOH and rTyrOH; the BH_2 hydroxyl groups in the hTrpOH structure have a dihedral angle of 40°, imposed by the adjacent residues Pro238 and Tyr312. In hTrpOH, both dihydroxypropyl hydroxyl groups hydrogen bond to a well-defined water molecule at equivalent distances (2.8 Å), and the dihydroxypropyl side chain 2′-OH atom also has a long hydrogen bond (3.3 Å) to the carbonyl oxygen of Ala309. Pro238 is one of a few major sequence differences at the pterin binding site in the AAOHs. The nonconserved nature of this residue may be useful in the design of cofactor analogues that can selectively modulate the biosynthesis of the monoamine neurotransmitters.

CONCLUSIONS

The first crystal structure of a truncated form of tryptophan hydroxylase as presented herein provides a major step toward defining a receptor/pharmacophore for reduced pteridines that can be used to develop more potent BH_4 analogue cofactors. Comparative structural analysis of the three pterin-dependent hydroxylases, in combination with biochemical analysis of additional AAOH−small molecule cocomplexes using substrate analogues and analogues of molecular oxygen, will

aid in the understanding of the catalytic mechanisms and determinants of substrate specificity for the family of AAOHs. In this fashion, activating BH_4 cofactor-type compounds and inhibiting substrate analogues can be developed to provide increased selectivity for enhancing serotonergic, noradrenergic, and/or dopaminergic function.

ACKNOWLEDGMENT

We thank Mary Straub and Sidsel Riise for expert technical assistance, Xiaoping Dai, Ph.D., for processing the data, and Marianne G. Patch, Ph.D., for help in manuscript preparation.

SUPPORTING INFORMATION AVAILABLE

Ramachandran plot for, *B*-factor plot for, representative electron density of, and a stereoview of the active site of hTrpOH. This material is available free of charge via the Internet at http://pubs.acs.org.

REFERENCES

1. Martinez, A., Knappskog, P. M., and Haavik, J. (2001) *Curr. Med. Chem. 8*, 1077−1091.
2. Abbar, M., Courtet, P., Bellivier, F., Leboyer, M., Boulenger, J. P., Castelhau, D., Ferreira, M., Lambercy, C., Mouthon, D., Paoloni-Giacobino, A., Vessaz, M., Malafosse, A., and Buresi, C. (2001) *Mol. Psychiatry 6*, 268−273.
3. Bell, C., Abrams, J., and Nutt, D. (2001) *Br. J. Psychiatry 178*, 399−405.
4. Kim, S. W., Park, S. Y., and Hwang, O. (2002) *Mol. Pharmacol. 61*, 778−785.
5. Stokes, A. H., Xu, Y., Daunais, J. A., Tamir, H., Gershon, M. D., Butkerait, P., Kayser, B., Altman, J., Beck, W., and Vrana, K. E. (2000) *J. Neurochem. 74*, 2067−2073.
6. Zimmer, L., Luxen, A., Giacomelli, F., and Pujol, J. F. (2002) *Neurochem. Res. 27*, 269−275.
7. Kapatos, G., and Kaufman, S. (1981) *Science 212*, 955−956.
8. Vanhoutte, P. M., Ed. (1985) *Serotonin and the vascular system*, Raven Press, New York.
9. Ekwall, O., Hedstrand, H., Grimelius, L., Haavik, J., Perheentupa, J., Gustafsson, J., Husebye, E., Kampe, O., and Rorsman, F. (1998) *Lancet 352*, 279−283.
10. Talley, N. J. (2001) *Lancet 358*, 2061−2068.
11. Goodwill, K. E., Sabatier, C., Marks, C., Raag, R., Fitzpatrick, P. F., and Stevens, R. C. (1997) *Nat. Struct. Biol. 4*, 578−585.
12. Goodwill, K. E., Sabatier, C., and Stevens, R. C. (1998) *Biochemistry 37*, 13437−13445.
13. Fusetti, F., Erlandsen, H., Flatmark, T., and Stevens, R. C. (1998) *J. Biol. Chem. 273*, 16962−16967.
14. Erlandsen, H., Fusetti, F., Martinez, A., Hough, E., Flatmark, T., and Stevens, R. C. (1997) *Nat. Struct. Biol. 4*, 995−1000.
15. Erlandsen, H., Flatmark, T., Stevens, R. C., and Hough, E. (1998) *Biochemistry 37*, 15638−15646.
16. Erlandsen, H., Bjørgo, E., Flatmark, T., and Stevens, R. C. (2000) *Biochemistry 39*, 2208−2217.
17. Kobe, B., Jennings, I. G., House, C. M., Michell, B. J., Goodwill, K. E., Santarsiero, B. D., Stevens, R. C., Cotton, R. G. H., and Kemp, B. E. (1999) *Nat. Struct. Biol. 6*, 442−448.
18. Erlandsen, H., Kim, J. Y., Patch, M. G., Han, A., Volner, A., Abu-Omar, M. M., and Stevens, R. C. (2002) *J. Mol. Biol. 320*, 645−661.
19. McKinney, J., Teigen, K., Frøystein, N. A., Salaun, C., Knappskog, P. M., Haavik, J., and Martinez, A. (2001) *Biochemistry 40*, 15591−15601.
20. Moran, G. R., Daubner, S. C., and Fitzpatrick, P. F. (1998) *J. Biol. Chem. 273*, 12259−12266.
21. Otwinowski, Z., and Minor, W. (1997) Processing of X-ray Diffraction Data Collected in Oscillation Mode, in *Methods in Enzymology* (Carter, C. W., Jr., and Sweet, R. M., Eds.) Vol. 276, pp 307−326, Academic Press, New York.
22. Kissinger, C. R., Gehlhaar, D. K., and Fogel, D. B. (1999) *Acta Crystallogr. D55*, 484−491.
23. Brunger, A. T., Adams, P. D., Clore, G. M., DeLano, W. L., Gros, P., Grosse-Kunstleve, R. W., Jiang, J. S., Kuszewski, J., Nilges, M., Pannu, N. S., Read, R. J., Rice, L. M., Simonson, T., and Warren, G. L. (1998) *Acta Crystallogr. D54*, 905−921.
24. Jones, T. A., Zou, J.-Y., Cowan, S. W., and Kjeldgaard, M. (1991) *Acta Crystallogr. A47*, 110−119.
25. Lu, G. (2000) *J. Appl. Crystallogr. 33*, 176−183.
26. Daubner, S. C., Moran, G. R., and Fitzpatrick, P. F. (2002) *Biochem. Biophys. Res. Commun. 292*, 639−641.
27. Daubner, S. C., Melendez, J., and Fitzpatrick, P. F. (2000) *Biochemistry 39*, 9652−9661.
28. Lovenberg, W., Jequier, E., and Sjoerdsma, A. (1967) *Science 155*, 217−219.
29. Kappock, T. J., and Caradonna, J. P. (1996) *Chem. Rev. 96*, 2659−2756.
30. Almås, B., Toska, K., Teigen, K., Groehn, V., Pfleiderer, W., Martinez, A., Flatmark, T., and Haavik, J. (2000) *Biochemistry 39*, 13676−13686.
31. Andersen, O. A., Flatmark, T., and Hough, E. (2001) *J. Mol. Biol. 314*, 279−291.
32. Jiang, G. C. T., Yohrling, G. J., Schmitt, I. V. J. D., and Vrana, K. E. (2000) *J. Mol. Biol. 302*, 1005−1017.
33. Kabsch, W., and Sander, C. (1983) *Biopolymers 22*, 2577−2637.

BI026561F